JOURNAL OF Materials CHEMISTRY

Synthesis, crystal structure and solid state NLO properties of a new chiral bis(salicylaldiminato)nickel(II) Schiff-base complex in a nearly optimized solid state environment

Frédéric Averseng,[a] Pascal G. Lacroix,*[a] Isabelle Malfant,[a] Françoise Dahan[a] and Keitaro Nakatani[b]

[a]*Laboratoire de Chimie de Coordination du CNRS, 205 route de Narbonne, 31077 Toulouse, France. E-mail: pascal@lcc-toulouse.fr*
[b]*PPSM, Ecole Normale Supérieure de Cachan, Avenue du Président Wilson, 94235 Cachan, France*

Received 18th October 1999, Accepted 4th January 2000

A new chiral ligand based on the condensation of 4-diethylaminosalicylaldehyde with (1*R*,2*R*)-(+)-1,2-diphenylethylenediamine (H_2L^2) is reported along with its nickel(II) complex. The diamagnetic NiL^2 complex exhibits an efficiency 13 times that of urea in second harmonic generation at 1.9 μm. The structure–property relationships are discussed on the basis of the crystal structure, in relation with that of a previously reported derivative which possesses the same molecular NLO response, but very different crystal structure.

Introduction

Molecular materials have emerged in many areas of material science for the design of new magnets,[1] assemblies for data storage,[2] conductors and superconductors,[3] or non-linear optical (NLO) materials.[4–6] One of the most promising features of molecular chemistry is the opportunity provided to modify and eventually optimize the stacking (and hence the solid state properties) through subtle modifications achieved at the molecular level. The purpose of the present contribution is to illustrate this versatility in the case of NLO Schiff-base complexes.

It has long been recognized that molecular chromophores could exhibit second-order NLO responses several orders of magnitude higher than that of the best inorganic compounds commercially available, such as $LiNbO_3$ or KH_2PO_4.[7] The search for molecular chromophores has mostly focused on organic systems,[4a,c] and organometallic molecules.[8] Nevertheless, several studies have revealed that inorganic complexes could have sizeable molecular hyperpolarizabilities (β),[9–14] Moreover, the introduction of a metal center may bring about NLO materials with additional characteristics such as electrochemical[15] and magnetic properties.[1a]

We, and others, have observed that bis(salicylaldimino)nickel(II) Schiff-base complexes could exhibit sizeable hyperpolarizabilities.[16,17] However, the tendency for crystal centrosymmetry leads to vanishing NLO response in the solid state. To overcome this difficulty, we have recently reported on a chiral complex NiL^1, which crystallizes in a non-centrosymmetric space group $P2_1$.[17b] The efficiency of NiL^1 in second harmonic generation (SHG) was very modest, for reasons related to pseudo-centrosymmetric stacking of the chromophores in the crystal. In a research effort aiming at optimizing the bulk non-linearity, we now extend our investigations to related chiral nickel(II) complexes having the same π-electronic structure, but different substituents to check the effect of the chiral core on the crystal packing. We report here on a comparison of two compounds NiL^1 and NiL^2. After checking that their molecular NLO responses (β) are similar, we try to find a rationale for understanding the different solid state properties from the molecular geometry.

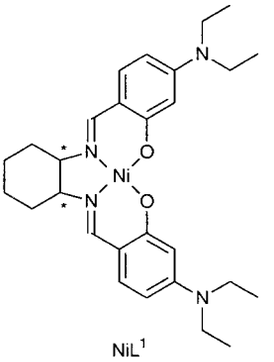

NiL^1

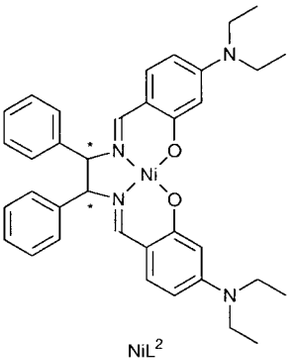

NiL^2

Experimental

Materials and equipment

NiL^1 was synthesized as previously reported.[17b] (1*R*,2*R*)-(+)-1,2-diphenylethylenediamine and $NiCl_2 \cdot 6H_2O$ were purchased from Fluka and used as received, as was 4-(diethylamino)-salicylaldehyde (Lancaster). Solvents (SDS or Carlo Erba) for the spectroscopic studies were used without further purification. ^1H NMR spectra were recorded on a Brucker AM 250 spectrometer, the UV-visible spectra on a Hewlett Packard 8452 A spectrophotometer and the specific rotations on a Perkin-Elmer 241 polarimeter. Elemental analyses were

DOI: 10.1039/a910244m

performed by the Service de Microanalyses du C.N.R.S., Laboratoire de Chimie de Coordination, Toulouse.

Synthesis of H_2L^2 and NiL^2

H_2L^2. 4-(Diethylamino)salicylaldehyde (776 mg, 4×10^{-3} mol) was added to a solution of 425 mg (2×10^{-3} mol) of (1*R*,2*R*)-(+)-1,2-diphenylethylenediamine in 50 ml of absolute ethanol. The solution was heated under reflux for one day, then concentrated and cooled to −20 °C. The pale yellow precipitate was filtered off, washed with cold ethanol, and dried under vacuum (yield 85%) (Found: C, 76.77; H, 7.52; N, 9.96. $C_{36}H_{42}N_4O_2$ requires C, 76.51; H, 7.44; N, 9.79%). ^{1}H NMR ($CDCl_3$): δ 1.143 (t, J=7.0, 12 H), 3.325 (q, J=7.0, 8H), 4.581 (s, 2H), 6.082 (dd, J=2.4, 8.6, 2H), 6.138 (d, J=2.4, 2H), 6.903 (d, J=8.6 Hz, 2H), 7.14 (m, 10H) and 8.048 (s, 2H).

NiL^2. In 50 ml of absolute ethanol were successively added 106 mg (5×10^{-4} mol) of (1*R*,2*R*)-(+)-1,2-diphenylethylenediamine, 119 mg (5×10^{-4} mol) of $NiCl_2\cdot6H_2O$, and 193 mg (10^{-3} mol) of 4-(diethylamino)salicylaldehyde. After a 16 h reflux, the resulting dark solution was slowly evaporated at room temperature. NiL^2 was obtained as red single crystals (yield 60%) (Found: C, 70.13; H, 6.04; N, 8.77. $C_{36}H_{40}N_4NiO_2$ requires C, 69.80; H, 6.51; N, 9.04%). ^{1}H NMR ($CDCl_3$): δ 1.123 (t, J=7.0, 12 H), 3.293 (q, J=7.0, 8H), 4.218 (s, 2H), 5.958 (dd, J=2.3, 8.9, 2H), 6.250 (d, J=2.3, 2H), 6.707 (d, J=8.9 Hz, 2H), 6.913 (s, 2H), 7.30–7.43 (m, 6H) and 7.97–8.01 (m, 4H). $\alpha=+1276°$ (EtOH, Na lamp, 589 nm, 20 °C).

X-Ray data collection and structure determination

The structure was solved by the Patterson method, using SHELXS 86.[18] The refinement was performed on F^2, using SHELXS 93.[19] Crystallographic data are summarized in Table 1. The drawings of the molecular structures were obtained with the help of CAMERON.[20] The atomic scattering factors were taken from ref. 21. The absolute configuration was determined, with a Flack coefficient equal to 0.01(2).

CCDC 1145/202. See http://www.rsc.org/suppdata/jm/a9/a910244m/ for crystallographic files in .cif format.

Calculation of the NLO response

The all-valence INDO/S (intermediate neglect of differential overlap) method[22] in connection with the sum-over-state (SOS) formalism[23] was employed. Details on the computationally efficient INDO–SOS-based method for describing second-order molecular optical non-linearities have been reported elsewhere.[24] The calculation of electronic transitions and molecular hyperpolarizabilities was performed using the commercially available MSI software package INSIGHT II (4.0.0).[22c] In the present approach, the closed-shell restricted Hartree–Fock (RHF) formalism was employed. The mono-excited configuration interaction (MECI) approximation was used to describe the excited states. The 100 energy transitions between the ten highest occupied molecular orbitals and the ten lowest unoccupied ones were chosen to undergo CI mixing. Metrical parameters used for the calculations were taken from the present crystal structure for NiL^2 and from the previously reported one for NiL^1.

Table 1 Crystal data for NiL^2

Formula	$C_{36}H_{40}N_4NiO_2$
M	619.43
Crystal system	Monoclinic
Space group	$P2_1$
a/Å	13.660(2)
b/Å	10.601(2)
c/Å	12.340(2)
β/°	112.09(1)
V/Å^3	1655.7
T/K	293
Z	2
Reflections collected	6127
Independent reflections	5842
R(int)	0.0163
μ(Mo-Kα)cm^{-1}	6.22
R	0.0352
wR	0.0632

NLO measurements

The measurements of SHG intensity were carried out by the Kurtz–Perry powder technique,[25] using a nanosecond Nd-YAG pulsed (10 Hz) laser. The fundamental beam (1.064 μm) was focused in a hydrogen cell (1 m long, 50 atm) and the outcoming Stokes-shifted radiation generation at 1.907 μm used as the fundamental beam for SHG. The SHG signal was detected by a photomultiplier and read on an ultrafast Tektronic TDS 620B oscilloscope. Samples were calibrated microcrystalline powders obtained by grinding, and put between two glass plates.

Results and discussion

Synthesis and characterization

The synthesis of Schiff-base complexes based on chiral 1,2-diamines is well documented for its applications in catalytic asymmetric synthesis.[26] The synthesis of H_2L^2 can be monitored by ^{1}H NMR spectroscopy to verify the disappearance of the CHO signal located at 9.47 ppm in the starting 4-(diethylamino)salicylaldehyde, and the appearance of the imine signal at 8.05 ppm (*versus* 7.92 ppm for H_2L^1).

Structure description

The molecular structure of NiL^2 and atom-labeling scheme are shown in Fig. 1. Except for the ethyl substituents of the amines and for the diphenylethylene fragments, the molecule is nearly planar. In particular, the nickel lies in an almost perfect square-planar coordination environment with largest deviation from the mean plane of 0.039 Å observed at O(2). Two molecules are present in the cell, related by a helicoidal 2_1 axis along b. For comparison with NiL^1, which crystallizes in the same space group, the Ni–O and Ni–N distances are given in Table 2 for both complexes. The coordination spheres are nearly identical with metal–ligand mean distances of 1.846(4) and 1.847(3) Å for NiL^1 and NiL^2 respectively. This indicates that the steric effect of the phenyl substituents in NiL^2 does not modify the π and d electronic core of the molecule. Therefore, the differences

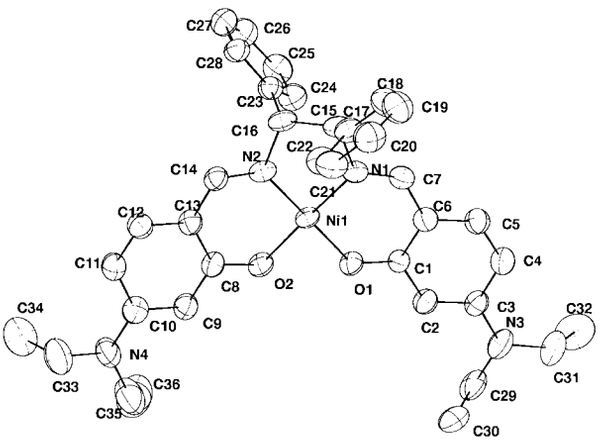

Fig. 1 Asymmetric unit and atom labeling scheme for NiL^2. H atoms are omitted for clarity.

Table 2 Selected bond lengths (Å) and angles (deg) for NiL^1 and NiL^2 with e.s.d.s in parentheses

	NiL^1	NiL^2
Ni–O(1)	1.850(3)	1.853(2)
Ni–O(2)	1.836(3)	1.840(2)
Ni–N(1)	1.861(4)	1.848(3)
Ni–N(2)	1.835(4)	1.846(3)
O(1)–Ni–O(2)	84.3(1)	84.2(1)
O(1)–Ni–N(1)	94.7(2)	94.9(1)
O(1)–Ni–N(2)	173.0(1)	177.8(1)
O(2)–Ni–N(1)	175.7(2)	177.3(1)
O(2)–Ni–N(2)	95.5(1)	95.0(1)
N(1)–Ni–N(2)	86.1(2)	86.0(1)

observed in the bulk NLO responses of the two chromophores should arise from different packings only.

Spectroscopic properties

The optical absorption spectra of H_2L^2 and NiL^2, recorded in ethanol, are shown in Fig. 2. The spectra exhibit an intense band at 342 ($\varepsilon_{max}=53\,400$) and 368 nm ($\varepsilon_{max}=44\,500$ dm^3 mol^{-1} cm^{-1}) for H_2L^2 and NiL^2, respectively. The general trend for a red shift upon metal complexation is observed for NiL^2 as previously reported.[16,17] For comparison, the spectrum of NiL^1 is also provided. Interestingly, it can be observed that both complexes exhibit the same spectroscopic features with an intense absorption ($\lambda_{max}=359$ nm, $\varepsilon_{max}=40\,700$ dm^3 mol^{-1} cm^{-1} for NiL^1), with additional less intense bands at higher and lower energy.

The absorption maxima recorded in solvents of different polarities are gathered in Table 3 for NiL^1 and NiL^2. A negative solvatochromism (blue shift in solvents of higher polarity) is observed in both cases. The behavior seems to be a trend in donor–acceptor salen complexes.[16,17] Moreover, it must be emphasized that solvatochromism is usually associated to changes in dipole moments between the ground and the excited states upon excitation ($\Delta\mu<0$ in the case of negative solvatochromism). Therefore, large dipole moment changes are strongly indicative of large quadratic hyperpolarizabilities (β) (see below). On the basis of such observations, solvatochromism has been suggested as a possible route for estimating molecular hyperpolarizabilities.[27] Therefore, it is interesting to compare the extent of solvatochromic shifts for NiL^1 and NiL^2. A large number of scales have been established to quantify the influence of the solvent based on some physicochemical properties.[28] The Reichardt parameter (E_T^N),[29] which is based on absorption spectroscopy of "push-pull" conjugated molecules, seems to be a suitable solvent polarity parameter, if NLO responses have to be considered. The energies of the absorption maxima are plotted *versus* (E_T^N) in Fig. 3. The

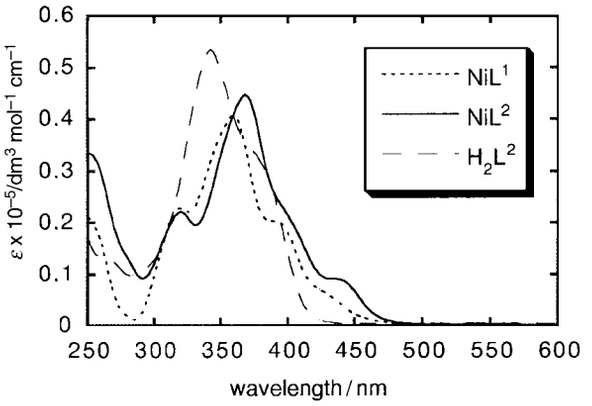

Fig. 2 Optical spectra for NiL^1, NiL^2 and H_2L^2 recorded in ethanol.

Table 3 Absorption maxima of the high intensity optical transition for compounds NiL^1 and NiL^2, recorded in solvents of different polarities (E_T^N, Reichardt parameter)

	λ_{max}/nm		
Solvent	NiL^1	NiL^2	E_T^N
MeOH	358	368	0.765
EtOH	359	368	0.654
MeCN	358	369	0.472
DMF	359	368	0.404
Acetone	360	368	0.355
Ethyl acetate	361	370	0.577
DMSO	361	371	0.441
THF	362	370	0.207
2-Propanol	362	368	0.552
CH_2Cl_2	363	373	0.321
Pyridine	364	372	0.293
$CHCl_3$	366	376	0.259
Toluene	366	375	0.096
CCl_4	370	377	0.090

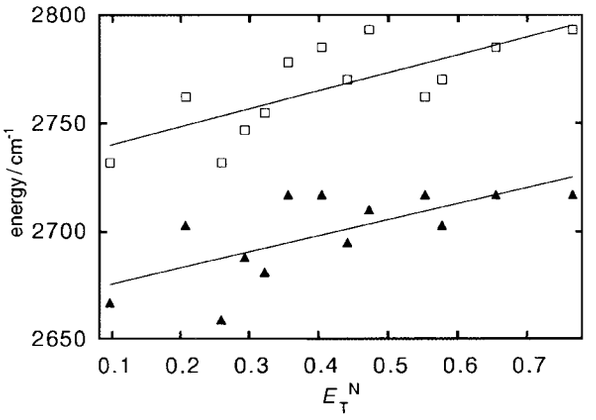

Fig. 3 Solvatochromism of NiL^2 (black triangles) *versus* that of NiL^1 (white squares).

slopes, which are equal to 82.6 and 74.3 cm^{-1}, for NiL^1 and NiL^2 respectively, suggest similar solvatochromic shifts, and probably similar $\Delta\mu$, as NiL^1 and NiL^2 are related molecules. Consequently, spectroscopy provides evidence for charge transfer transitions with similar intensities (ε and oscillator strength f),[30] similar energies (ΔE), and similar changes in dipole moments ($\Delta\mu$) for both nickel complexes. On the basis of the rough two-level description of the quadratic non-linearity ($\beta\propto\Delta\mu\times f/(\Delta E)^3$),[31] we may infer that the molecular hyperpolarizabilities of NiL^1 and NiL^2 are similar.

These observations can be compared to the Zerner INDO (ZINDO) derived spectroscopic properties gathered in Table 4. There is a significant difference in λ_{max} between calculation and experiment, but it lies in the range of uncertainties previously reported for ZINDO calculations of nickel complexes.[16,17] The point of interest in Table 4 is that experiment and calculation indicate that NiL^1 and NiL^2 should exhibit similar molecular optical non-linearities. This will be verified in the next section.

Table 4 Experimental and ZINDO-computed data for the high intensity optical transition of NiL^1 and NiL^2

	λ_{max}/nm		Intensity		$\Delta\mu$/D
Compound	Calc.	Exp.	Calc.(f)	exp.(ε/dm^3 mol^{-1} cm^{-1})	calc.
NiL^1	324	359	0.62	40700	−7.0
NiL^2	312	368	0.55	44500	−7.5

Table 5 Molecular hyperpolarizabilities[a] at various wavelengths in 10^{-30} cm^5 esu^{-1}, for NiL^1 and NiL^2

	NiL^1		NiL^2	
Wavelength/μm	β_{total}	(β_{2level})	β_{total}	(β_{2level})
∞	−17.5	(−20.4)	−18.8	(−25.1)
1.907	−20.5	(−23.2)	−21.8	(−28.3)
1.064	−32.6	(−34.2)	−32.8	(−39.3)

[a] $\beta=\sqrt{\beta_x^2+\beta_y^2+\beta_z^2}$ with $\beta_i=\beta_{ixx}+\beta_{iyy}+\beta_{izz}$. β_{xxx} (x being the charge transfer axis) represents 50% of β.

NLO properties of NiL^2 *versus* NiL^1

Details for the β calculations for both NiL^1 and NiL^2 are provided in Table 5. In particular, the trend for β enhancement at higher frequencies is observed, as the second harmonic becomes closer to the electronic transitions of the chromophores. The calculation reveals that the hyperpolarizabilities are extremely similar for NiL^1 and NiL^2, as anticipated from the spectroscopic data discussed in the previous section. The two-level terms (β_{2level})[24] dominate the non-linearity for both chromophores. In the case of NiL^2, it can mainly be related to the 1→6 transition (29%), which corresponds to λ_{max}. Therefore, we make the assumption that understanding this transition will provide quantitative understanding of β. The differences in electronic population in the dominant transition involved in the NLO responses of NiL^1 and NiL^2 are compared in Fig. 4, which illustrates the similarities between the charge transfer, and hence the molecular NLO response, for the two materials.

The NLO properties of the crystals recorded as the SHG efficiencies are gathered in Table 6. The results clearly show a trend for higher values as the size of the particles increases with intensities up to 13 times that of urea for NiL^2. This tendency indicates that the crystals are phase matchable,[25a] a situation highly desirable for practical use of the compound as a single crystal. At first, it may be surprising that NiL^1 and NiL^2, which have the same β, exhibit so different SHG efficiencies in the solid state, NiL^2 being 30 times (9 *vs.* 0.3) more efficient than NiL^1.

The hyperpolarizability tensor (components β_{ijk} in the molecular framework) is related to the corresponding crystalline first-order non-linearity $\chi^{(2)}$ (components d_{IJK} in the crystalline framework).[32] Assuming a one-dimensional character of the molecular non-linear tensor of the molecules, β has only one large coefficient along the charge transfer axis x of the molecule (namely β_{xxx}). NiL^2 crystallizes in space group $P2_1$, which leads to the relations (1) and (2).[33,34]

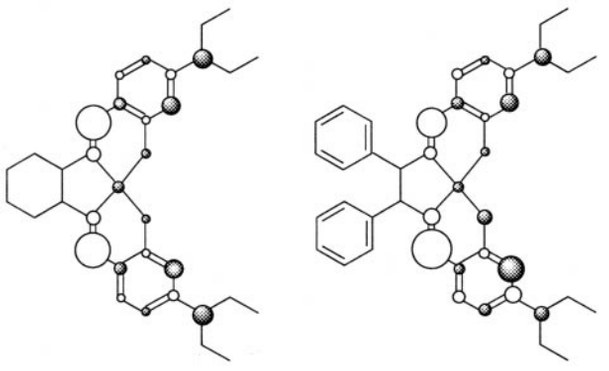

Fig. 4 Difference in electronic populations between ground and excited state for the main transition (1→6) involved in the NLO response of NiL^1 and NiL^2 (data from ref. 17(b) for NiL^1). The white (shaded) contribution is indicative of an increase (decrease) of electron density in the charge transfer process.

Table 6 Comparison of the powder efficiencies in second harmonic generation ($I_{2\omega}$) for NiL^1 and NiL^2 *versus* that of urea

Compound	Grain caliber/μm	Powder efficiency
Urea	50–80	1 (reference)
NiL^1	50–80	0.3
NiL^2	50–80	9
	80–125	11.5
	125–180	13

$$d_{ZXX}=N\beta_{xxx}\cos\theta\sin^2\theta \quad (1)$$

$$d_{ZZZ}=N\beta_{xxx}\cos^3\theta \quad (2)$$

All other components of the tensor are weak (θ is defined as the angle between the resulting molecular charge transfer axis 0x and the twofold axis 0Z of the crystal). The optimization of d_{ZZZ} can be achieved with $\theta=0°$, a situation which is of no use for birefringence phase matching, and must therefore be avoided. More importantly, the angular factor weighting β_{xxx} in the expression of d_{ZXX} is maximized and equal to 0.385 for $\theta=54.74°$. Any phase-matching configuration emphasizing this coefficient is to be considered as highly desirable. The orientation of β in the crystal cell is shown in Fig. 5, for NiL^2. θ reaches a value of 57.8° and an angular factor of 0.381, which indicates that the orientation of the molecule is nearly optimized. With the above consideration, we can infer that an SHG efficiency 13 times that of urea is close to the upper limit in this class of bis[(4-diethylamino)salicylaldiminato]metal Schiff-base complexes.

By contrast, we can measure an angle of 178.3° between the resulting charge transfer axis of the two non-equivalent molecules of the asymmetric unit cell of NiL^1.[17b] This leads to cancellation of 97% of the NLO response. Any orientation of the resulting β with respect to the twofold axis will further reduce the properties and about 1% of the individual molecular non-linearity will contribute to the crystalline NLO coefficient, *versus* 38% in NiL^2. It is therefore not surprising that the SHG efficiency of NiL^1 is much lower than that of NiL^2.

Chirality bulk-properties relationships in Ni(salen) complexes

It is well known that crystal geometries are unpredictable from gas phase molecular geometries.[35] However, a statistical search conducted on every reported structure of monomeric species containing the *N*,*N*′-bis(salicylidene)ethylenediaminonickel(II) skeleton reveals that only two structures in about 25 entries actually are non-centrosymmetric.[36,37] Moreover, these struc-

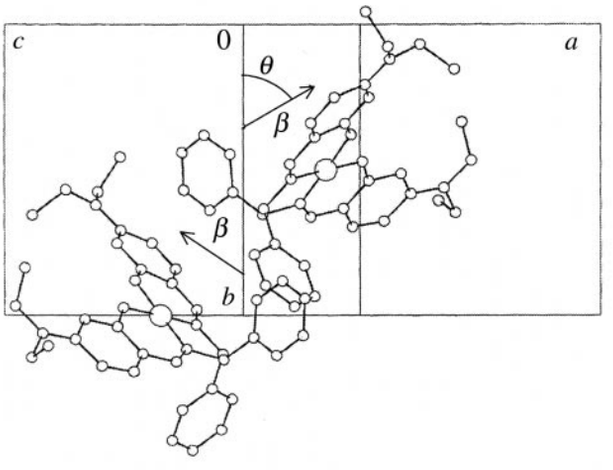

Fig. 5 CAMERON view of NiL^2 showing the angle ($\theta=57.8°$) between β and the C_2 helicoidal axis.

tures were obtained with chiral substituents. Therefore, molecular chirality seems to be the key for observing non-zero SHG efficiencies in these compounds.

In spite of the above considerations, it would be interesting to find a rationale for the difference in the crystal structures (and hence SHG efficiencies) between NiL^1 and NiL^2, by means of a molecular parameter related to the concept of chirality. For instance, it seems natural to consider the angle of optical rotation α. We have measured values of $+1276^\circ$ for NiL^2, *versus* -1050° for NiL^1. These results lying in the same range of magnitude ($\pm 20\%$) indicate that the optical activity cannot explain the difference in the magnitude of the SHG efficiencies. A better approach would be to compare and try to quantify some structural features of the molecules. In the case of NiL^2 it is clear that two enantiomers made from (1*R*,2*R*)-(+)-1,2-diphenylethylenediamine and (1*S*,2*S*)-(−)-1,2-diphenylethylenediamine are very different molecules. By contrast, two enantiomers of NiL^1 made from (1*R*,2*R*)-(−)-1,2-diaminocyclohexane and (1*S*,2*S*)-(+)-1,2-diaminocyclohexane could be placed upon each other in such a way that a large part of them coincides. This difference is emphasized in Fig. 6, where the projections of NiL^1 and NiL^2 along the mean plane of the molecules are compared. The figure reveals that the out of plane displacement of the chiral substituents is large in NiL^2. A calculation indicates that the centroids of the phenyl substituents are located 3.06 and 3.31 Å apart from the Ni(1)–N(1)–N(2) plane of the molecules, which can account for an enhanced "degree of chirality".[38] By contrast, the cyclohexyl group lies close to the molecular plane of NiL^1, with an averaged distance between the carbons of the cyclohexyl and the Ni(1)–N(1)–N(2) plane equal to 0.31 Å. This proximity indicates that the (1*R*,2*R*) and (1*S*,2*S*) isomers placed upon each other could overlap almost perfectly, since the overall diameters of the molecules are roughly identical. Consequently, the degree of chirality is higher in NiL^2 than in NiL^1, and it is therefore not surprising that the highest SHG efficiency is obtained in NiL^2. Using chiral substituents with large sizes and large out of plane displacements appears to be the key towards asymmetric arrangements of metal salen chromophores in the crystal structure.

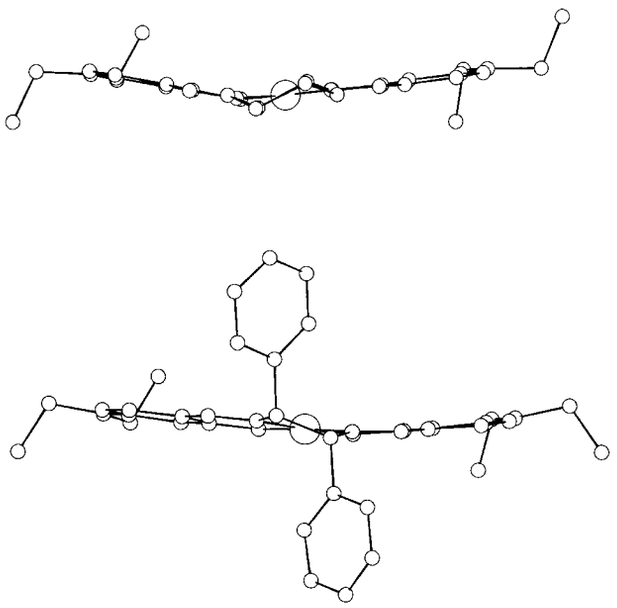

Fig. 6 Projections along the mean planes of the molecules for NiL^1 (top) and NiL^2 (bottom).

Conclusion

We have discussed the structure–property relationship in a class of chiral Schiff-base nickel(II) metal complexes. The compounds under investigation possess the same charge transfer π-electronic core, which indicates related molecular properties and potential application as NLO chromophores. In particular, NiL^2 is the most SHG efficient bis(salicylaldiminato)metal Schiff-base complex reported to date. The chiral substituents, which are innocent in the charge transfer process, play the major role for engineering the molecules in different non-centrosymmetric solid state environments, which, in the case of NiL^2, results in a crystal packing nearly optimized for NLO purposes.

References

1 (*a*) O. Kahn, *Molecular Magnetism*, VCH, Weinheim, 1993; (*b*) J. S. Miller and A. J. Epstein, *Angew. Chem., Int. Ed. Engl.*, 1994, **33**, 385.
2 O. Kahn and C. J. Martinez, *Science*, 1998, **279**, 44.
3 P. Cassoux and J. S. Miller, in *Chemistry of Advanced Materials: An Overview*, eds. L.V. Interrante and M. J. Hampden-Smith, Wiley-VCH, Inc., New York, 1998, p. 19.
4 (*a*) *Nonlinear Optical Properties of Organic Molecules and Crystals*, eds. S. Chemla and J. Zyss, Academic Press, New York, 1987; (*b*) *Molecular Nonlinear Optics*, ed. J. Zyss, Academic Press, New York, 1994; (*c*) *Nonlinear Optics of Organic Molecules and Polymers*, eds. H. S. Nalwa and S. Miyata, CRC Press, New York, 1997.
5 *Optical Nonlinearities in Chemistry*, special issue of *Chem. Rev.*, 1994, **94**.
6 *Nonlinear Optical Properties of Organic Materials, Proc. SPIE*, 1988–1994, **971**, **1147**, **1337**, **1560**, **1775**, **2025**, **2285**.
7 D. J. Williams, *Angew. Chem., Int. Ed. Engl.*, 1984, **23**, 690.
8 For recent reviews on NLO organometallics see: N. L. Long, *Angew. Chem., Int. Ed. Engl.*, 1995, **34**, 21; S. R. Marder, in *Inorganic Materials*, eds. D. W. Bruce and D. O'Hare, John Wiley & Sons, New York, 1992, p. 115; I. R. Whittall, A. M. McDonagh, M. G. Humphrey and M. Samoc, *Adv. Organomet. Chem.*, 1998, **42**, 291.
9 For a recent review, see: T. Verbiest, S. Houbrechts, M. Kauranen, K. Claes and A. Persoons, *J. Mater. Chem.*, 1997, **7**, 2175.
10 M. Bougault, C. Mountassir, H. Le Bozec, I. Ledoux, G. Pucetti and J. Zyss, *J. Chem. Soc., Chem. Commun.*, 1993, 1623.
11 J. Zyss, C. Dhénaut, T. Chauvan and I. Ledoux, *Chem. Phys. Lett.*, 1993, **206**, 409.
12 W. Chiang, D. M. Ho, D. Van Engen and M. E. Thompson, *Inorg. Chem.*, 1993, **32**, 2886.
13 S. M. Lecours, H.-W. Guan, S. G. Dimagno, C. H. Wang and M. J. Therien, *J. Am. Chem. Soc.*, 1996, **118**, 1497; S. Priyadarshy, M. J. Therien and D. N. Beratan, *J. Am. Chem. Soc.*, 1996, **118**, 1504.
14 S. D. Cummings, L. T. Cheng and R. Eisenberg, *Chem. Mater.*, 1997, **9**, 440.
15 G. L. Geoffroy and M. S. Wrighton, *Organometallic Photochemistry*, Academic Press, New York, 1979; J. P. Collman and L. S. Hegedus, *Principles and Applications of Organotransition Metal Chemistry*, University Science Books, Mill Valley, CA, 1987.
16 S. Di Bella, I. Fragalà, I. Ledoux, M. A. Diaz-Garcia, P. G. Lacroix and T. J. Marks, *Chem. Mater.*, 1994, **6**, 881; S. Di Bella, I. Fragalà, I. Ledoux and T. J. Marks, *J. Am. Chem. Soc.*, 1995, **117**, 9481; S. Di Bella, I. Fragalà, I. Ledoux, M. A. Diaz-Garcia and T. J. Marks, *J. Am. Chem. Soc.*, 1997, **119**, 9550.
17 (*a*) P. G. Lacroix, S. Di Bella and I. Ledoux, *Chem. Mater.*, 1996, **8**, 541; (*b*) G. Lenoble, P. G. Lacroix, J. C. Daran, S. Di Bella and K. Nakatani, *Inorg. Chem.*, 1998, **37**, 2158; (*c*) F. Averseng, P. G. Lacroix, I. Malfant, G. Lenoble, P. Cassoux, K. Nakatani, I. Maltey-Fanton, J. A. Delaire and A. Aukauloo, *Chem. Mater.*, 1999, **11**, 995.
18 G. M. Sheldrick, SHELXS 86, Program for Crystal Structure Solution, University of Göttingen, 1986.
19 G. M. Sheldrick, SHELXS 93, Program for the Refinement of Crystal Structure from Diffraction Data; University of Göttingen; 1993.
20 D. J. Watkin, C. K. Prout and L. J. Pearce, CAMERON,

Chemical Crystallography Laboratory, University of Oxford, Oxford, 1996.
21 D. T. Cromer and J. T. Waber, *International Tables for X-Ray Crystallography*, Kynoch Press, Birmingham, 1974, vol. 4.
22 (*a*) M. C. Zerner, G. Loew, R. Kirchner and U. Mueller-Westerhoff, *J. Am. Chem. Soc.*, 1980, **102**, 589; (*b*) W. P. Anderson, D. Edwards and M. C. Zerner, *Inorg. Chem.*, 1986, **25**, 2728; (*c*) ZINDO, 96.0/4.0.0. Molecular Simulations Inc., 1996.
23 J. F. Ward, *Rev. Mod. Phys.*, 1965, **37**, 1.
24 D. R. Kanis, M. A. Ratner and T. J. Marks, ref. 5, p. 195.
25 (*a*) S. K. Kurtz and T. T. Perry, *J. Appl. Phys.*, 1968, **39**, 3798; (*b*) J. P. Dougherty and S. K. Kurtz, *J. Appl. Crystallogr.*, 1976, **9**, 145.
26 M. Palucki, P. J. Pospisil, W. Zhang and E. N. Jacobsen, *J. Am. Chem. Soc.*, 1994, **116**, 9333; J. F. Larrow and E. N. Jacobsen, *J. Am. Chem. Soc.*, 1994, **116**, 12129; E. N. Jacobsen, W. Zhang, A. R. Muci, J. R. Ecker and L. Deng, *J. Am. Chem. Soc.*, 1991, **113**, 7063.
27 M. S. Paley, J. M. Harris, H. Looser, J. C. Baumert, G. C. Bjorklund, D. Jundt and R. J. Twieg, *J. Org. Chem.*, 1989, **54**, 3774.
28 For a review of the solvent polarity scales, see: E. Buncel and S. Rajagopal, *Acc. Chem. Res.*, 1990, **23**, 226.
29 C. Reichardt and E. Harbusch-Görnet, *Liebigs Ann. Chem.*, 1983, **5**, 721.
30 M. Orchin and H. H. Jaffé, *Symmetry Orbitals, and Spectra*, John Wiley, New York, 1971, p. 204.
31 J. L. Oudar and J. Chemla, *J. Chem. Phys.*, 1977, **66**, 2664; J. L. Oudar, *J. Chem. Phys.*, 1977, **67**, 446.
32 J. Zyss and J. L. Oudar, *Phys. Rev. A*, 1982, **26**, 2028.
33 J. L. Oudar and J. Zyss, *Phys. Rev. A*, 1982, **26**, 2016.
34 J. Zyss, J. F. Nicoud and M. Coquillay, *J. Chem. Phys.*, 1984, **81**, 4160.
35 A. Gavezzotti, *Acc. Chem. Res.*, 1994, **27**, 309.
36 S. J. Wey, K. J. O'Conner and C. J. Burrows, *Tetrahedron Lett.*, 1993, 1905.
37 A. Wojtczak, E. Szlyk, M. Jaskolski and E. Larsen, *Acta Chem. Scand.*, 1997, **51**, 274.
38 For an introduction to the quantification of chirality, see: A. B. Buda, T. Auf der Heyde and K. Mislow, *Angew. Chem., Int. Ed. Engl.*, 1992, **31**, 989.

Paper a910244m